Radon Kinetics in a Basement Space Measured with Different Devices

Long Kiu Chung[1], Nathan P. Piersma[1], Kimberlee J. Kearfott[1]

Corresponding Author: Kimberlee J. Kearfott, Department of Nuclear Engineering and Radiological Sciences, University of Michigan, 2355 Bonisteel Boulevard, Ann Abor, Michigan, 48109 - 2104 USA

E-Mail: kearfott@umich.edu; Telephone: 1 (734) 763-9117; Fax: 1 (734) 763-4540

Conflicts of Interest and Sources of Funding: The only conflict of interest declared by the authors is the modest donation of RadonEyes (retailing at $180) for testing by RadonFTLabs. Funding was received from U.S. Department of Energy National Nuclear Security Administration and from the University of Michigan Fastest Path to Zero Initiative mini-grant and maker space programs.

Acknowledgements

Sungsoo Kim of RadonFTLab donated RadonEyes for testing. This work was funded in part by the Department of Energy National Nuclear Security Administration Consortium for Verification Technology award number DE-NA0002534 and Department of Energy National Nuclear Security Administration Consortium for Monitoring, Technology, and Verification award number DE-FOA-0001875. Additional support was received from the University of Michigan Fastest Path to Zero Initiative mini-grant and maker space programs, courtesy of Prof. Todd Allen. Mr. Jordan D. Noey supported laboratory operations.

Footnotes

[1] Department of Nuclear Engineering and Radiological Sciences, University of Michigan, Ann Arbor, MI 48109-2014, USA

Radon Kinetics in a Basement Space Measured with Five Different Devices

Abstract

Although indoor monitoring of radon and benchmarking of radon measurement devices remain important research topics, few intercomparisons of active radon measurement devices have been performed under realistic conditions, let alone dynamic ones enabling comparison of their transient behavior. Five different radon monitors were therefore placed in a poorly ventilated basement space under three different conditions: 24 h under a steady, elevated radon level, 24 h with fans turned on to produce a radon washout transient, and 9 d with fans turned off for a radon buildup transient. Resulting radon concentrations varied between ~200 and ~2,000 Bq m^{-3}. Accuracy of the devices were evaluated using root-mean-square error and ventilation data were fit to first order linear compartmental models. To more accurately model behaviors such as cyclic diurnal variations, the source term corresponding to entry of radon from soil into the basement was considered to be non-constant, as it is likely to vary drastically with both the indoor-outdoor pressure differential and soil concentration variations. The improved radon washout model fit very well with the measurements. Despite a wide variety in list prices, all devices performed similarly during transients and at different radon concentrations.

Keywords: Radon, radon monitors, ventilation, temporal measurements

Introduction

Radon, a collective term for ^{222}Rn, ^{220}Rn, and their progenies, is the single largest source of non-medical radiation exposure to the United States population (NCRP 2009), and the most common cause of lung cancer besides smoking (WHO 2009). With a much shorter half-life than ^{222}Rn, ^{220}Rn is often overlooked or neglected, the health hazard of which attributes almost entirely to its particulate progenies (Kanse et al. 2013). Radon releases into the air from the decay of radium in soil or building materials, often concentrating in the basement or other indoor spaces, with level as high as 410,000 Bq m^{-3} having been recorded in an occupied dwelling (Kearfott 1989). Indoor monitoring of radon is therefore a very important from the public health viewpoint.

Methods for such screening purposes often involve passive and active radon measurement devices (Keith et al. 2012). Passive integrating devices, such as charcoal canisters (Lehnert and Kearfott 2010) and alpha-track detectors (Ye et al. 2020), do not require power and produce a single measurement that corresponds to their deployment period. Active devices, such as ionization chambers and scintillation counters, provide temporal measurements which may enable a more comprehensive characterization of radon and its diurnal fluctuations. From low-cost, simple gadgets for screening to expensive, laboratory-grade monitors for research purposes, active radon monitoring devices vary in price, accuracy, sensitivity, dependence upon environmental conditions, and capability. Thorough analysis and comparison of different models of non-integrating active radon monitors under realistic and variable conditions would provide valuable information for consumers and researchers alike. However, published work intercomparing radon monitors, often focusing on integrating detectors or performed under laboratory conditions, is somewhat limited (Burghele and Cosma 2013; Cardellini et al. 2016; Gunning et al. 2016; Janik et al. 2010; Papp et al. 2016).

An unventilated basement space with a high, steady radon level, around 1,083 Bq m^{-3}, was discovered in a laboratory building (Xie et al. 2015, 2017). Carmona and Kearfott (2019) intercompared ten different active devices in that environment over a time period of roughly one month in that space. There were minimal transients during the experiment, with a slow trending increase in radon levels from ~500 to 2,000 Bq m^{-3} due to door openings, device equilibration, and introduction of ^{226}Ra dials. The results do not therefore reflect differences in radon monitor performance that could occur with rapid changes in the environment. Such changes could be anticipated because indoor radon concentration is heavily affected by variations in soil radon level and factors contributing to radon's entry into buildings. Pressure gradients, soil moisture, ground cover, humidity, soil and building material porosity, indoor and outdoor temperatures, and other factors could all contribute to such indoor radon transients (Lin et al. 2011; Turk et al. 1996; Yarmoshenko 2018; Kuo and Tsunomori 2014; Zafrir et al. 2013). Carmona and Kearfott (2019) also used the Coefficient of Determination (R^2) for their analysis. This is considered inappropriate for comparing measurements to a standard (Legates and McCabe 1999; Ritter and Munoz-Carpena 2013), although the standard was arbitrarily selected.

Chung et al. (2020) later conducted a series of experiments in the same basement space, developing equations that model the radon concentration with ventilation. However, experimental verifications were only performed using a single active radon monitor with long measuring intervals. To further verify the equations and to intercompare behaviors of different active devices under a transient condition, five radon monitors were placed in the basement space for this work, with fans turned on and off to observe relationships between measurements and compartmental models.

Methods

Selection of Radon Monitors for Investigation: In this study, intercomparisons were performed using a laboratory-grade radon monitor with pulsed-ionization chamber

(AlphaGUARD, Bertin Technologies, Parc d'activités du Pas du Lac, 10 bis, avenue Ampère, 78, 180 Montigny-le-Bretonneux, France), a Lucas-Cell-based radon detector (Model AB-5 with Model 300 and Model LCA-2, Pylon Electronics Inc., 147 Colonnade Rd, Nepean, Ontario, Canada K2E 7L9), two household systems with dual-structured pulsed-ionization chambers (RadonEye and RadonEye Plus2, RadonFTLab, 503ho, 8, 330gil, Haebong-ro, Danwon-gu, Ansan-city, Gyeonggido, South Korea), and a mitigatory-grade model with diffused-junction photodiodes (RadonSentinel, Model 1030, Sun Nuclear Corporation, 3257 Suntree Blvd., Melbourne, FL 32940). A summary of their price, memory, battery, accuracy, sensitivity, range, and measurement interval used, as reported by their manufacturers or a commercial laboratory (Bowser-Morner Inc., 4514 Taylorsville Road, Dayton, OH 45424), appears as Table 1.

Many other popular home-use devices, such as Corentium Home (Airthings, 25 N River Lane, Suite 406, Geneva, IL 60134), Canary (Airthings, 25 N River Lane, Suite 406, Geneva, IL 60134), or Pro Series3 (Sylvane Inc., 245 Hembree Park Drive, Suite 124, Roswell, GA 30076), are only capable of recording measurements at 24-h intervals, which are too sparse to capture any meaningful temporal changes in the experiment. They were therefore not included in this study.

Calibration and Steady-State Intercomparison: As shown in Fig. 1, the five devices were placed in the basement space at a height of 74 cm from the floor and at least 50 cm from walls to avoid leaked radon from the soil sources biasing the measurements, although the extent of which is likely trivial (Chung et al. 2020). The space was unventilated and separated from other rooms by double steel doors which contribute to the existence of a high and steady radon concentration. The devices were in position and turned on at least two hours before the experiment to allow radon to reach equilibrium within the devices. Lighting conditions remained constant throughout the experiment.

Steady-state measurements were taken over a 24-h period. Unfortunately, most of the devices used were aged beyond their official calibrations at the time of the experiment. To allow for a fair comparison, measurements from the AlphaGUARD, arbitrarily chosen as the "gold standard" radon monitor with zero error assumption (Carmona and Kearfott 2019). These measurements were used to linearly adjust the calibration of the other monitors using the following equation:

$$X = \frac{R_{AlphaGUARD}}{R_{device}} \tag{1}$$

where X is the calibration factor, $R_{AlphaGUARD}$ is the radon concentration measurement of AlphaGUARD in Bq m^{-3}, and R_{device} is the radon concentration measurement of the device in Bq m^{-3}, at the matching timestamp. If a device's measurement interval is different than that of the AlphaGUARD, the average $R_{AlphaGUARD}$ during such interval was used instead. The average X over the 24-hour period for each device, $\bar{X}$, was then multiplied with the corresponding R_{device} to obtain the re-calibrated readings.

To evaluate how well the measurements of the devices follow those of the AlphaGUARD, the root-mean-square error ($RMSE$) was used, defined as:

$$RMSE = \sqrt{\frac{\sum_{i=1}^{n}(R_{AlphaGUARD,i} - \bar{X}R_{device,i})^2}{n}} \tag{2}$$

where n is the number of measurements made by the device. Devices with different measuring interval were also handled by taking the average $R_{AlphaGUARD}$ over such interval.

Intercomparison with Ventilation: Five household box fans (Model 9723, Air King America, Limited Liability Company, 820 Lincoln Avenue, West Chester, PA 19380), with a flow rate of

3,770 m^3 h^{-1} as reported by manufacturer, were placed at the locations as shown in Fig. 1 and turned on for 24 h with the double steel doors open. The fans were then turned off with the double steel doors closed for 9 d. Lighting conditions remained constant.

When fans were turned off, the radon concentration buildup can be described by the following compartmental model (Chung et al. 2020):

$$\frac{\mathrm{d}R_{off}(t)}{\mathrm{d}t} = S_{off} - (L + \lambda)R_{off}(t) \tag{3}$$

where $R_{off}(t)$ is the radon concentration measurements during buildup in Bq m^{-3} as a function of time t in h, S_{off} is the chamber source term when the fans were turned off in Bq m^{-3} h^{-1}, L is the chamber leakage term in h^{-1}, and λ is the radon decay constant, 0.007554 h^{-1} (Lederer and Shirley 1978). Assume S_{off} and L to be constant, eqn (3) can be solved as:

$$R_{off}(t) = \frac{S_{off}}{\lambda + L} + e^{-(\lambda+L)t}(R_{off}(t_0) - \frac{S_{off}}{\lambda + L}) \tag{4}$$

where t_0 is the initial time in h. S_{off} and L were determined by curve-fitting the measurements to eqn (4) using a commercially available mathematics package format (MATLAB R2018b with Curve Fitting Toolbox, The Math-Works Inc., 3 Apple Hill Drive, Natick, MA 01760).

When fans were turned on in the prior work, Chung et al. (2020) assumed the source term is negligible, with radon concentration approaching zero as time goes to infinity. However, this was not true in the prior experiments, as the data only followed exhibited a negligible source term for the initial time period during a wash-out. A more realistically model for the situation is:

$$\frac{\mathrm{d}R_{on}(t)}{\mathrm{d}t} = S_{on} - (F + L + \lambda)R_{on}(t) \tag{5}$$

where $R_{on}(t)$ is the radon concentration measurements when fans were turned on in Bq m^{-3} as a function of time t in h, S_{on} is the chamber source term when the fans were turned on in Bq m^{-3}

h^{-1}, and F is the loss term from the fan in h^{-1}. Assume L to be carried over from eqn (4) and S_{on} and F to be constant, eqn (5) can be solved as:

$$R_{on}(t) = \frac{S_{on}}{\lambda + L + F} + e^{-(\lambda+L+F)t}\left(R_{on}(t_0) - \frac{S_{on}}{\lambda + L + F}\right) \tag{6}$$

where S_{on} and F can be determined similarly by curve-fitting.

Chung et al. (2020) also evaluated the goodness of fit for the models using reduced chi-squared characteristics. However, the associated errors were assumed as square root of the measurements, which did not take into account the sensitivity and calibration of the device. This does not invalidate the results and conclusions of that work, as only one radon monitor was involved in the study. A more realistic description of the errors (McGregor and Shultis 2020) and the reduced chi-squared statistics (Taylor 1997) of the devices is:

$$\chi_r{}^2 = \frac{\left[\sum_{i=1}^{n} \frac{\sqrt{sT}(y_i - f_i)}{\bar{X}\sqrt{y_i}}\right]^2}{n-2} \tag{7}$$

where $\chi_r{}^2$ is the reduced chi-squared characteristic, y is the actual radon concentration measurements of R_{on} or R_{off} in Bq m^{-3}, f is the modeled values according to eqn (4) or eqn (6) in Bq m^{-3}, s is the sensitivity of the device in cpm Bq^{-1} m^3, and T is the measurement interval of the device in min. Values of s and T can both be found on Table 1.

Similar to a steady-state intercomparison, agreements of the devices with the AlphaGUARD measurements were also quantified using the *RMSE*.

Results

Calibration and Steady-State Conditions: The calibrated radon concentration measurements by the five devices over the 24-h steady-state period are shown in Fig. 2a, with the corresponding $\bar{X}$ and *RMSE* appearing in Table 2.

Though chosen by Carmona and Kearfott (2019) and for this work as the "gold standard", the AlphaGUARD experienced significant fluctuations during measurements, even when compared with the AB-5, which has the same measuring interval. This is apparent in Fig. 2a. That said, when averaged over larger sampling times, as Carmona and Kearfott (2019) did, the AlphaGUARD measurements smoothen and follow closely with results from other devices. A similar phenomenon was observed by Tanaka et al. (2017), who compared AlphaGUARD with more sensitive and accurate monitoring devices under different steady-state conditions. Though the effect is thus unlikely due to actual changes in radon level, the exact cause, whether due to noise or sensitivity drift, requires further investigation, the result of which may challenge the "gold standard" assumption.

As shown on Table 2, despite being three years out of calibration, both the RadonEye and RadonEye Plus2 still boosted high accuracies, as evidenced by their $\bar{X}$ being very close to one. Just as observed by Carmona and Kearfott (2019), their measurements also agree very well with AlphaGUARD with low *RMSE*, even though their list prices are more than 50 times less. Although the RadonEye Plus2 is a newer model than the RadonEye, these two devices have no significant differences in design or operation.

Ventilation or Washout Conditions: Radon concentration measurements from the five devices are shown in Fig. 2b and Fig. 3 for buildup and Fig. 2c and Fig. 4 for washout. Their best-fit characteristics and *RMSE* are shown in Table 2.

The relative performance of the different radon monitors during the washout were similar to those observed under the steady-state conditions. The RadonEye and RadonEye Plus2 measurements vary closely with those of the AlphaGUARD. Similar to its steady-state measurements, the AlphaGUARD did experience significant fluctuations, especially at higher concentrations. Interestingly, RadonSentinel follows the predicted model the best during both radon buildup and washout, having its χ_r^2 closest to one out of all the devices.

Build-up Conditions: Despite the large number of data points, the predicted L and S_{off} from all devices fall very closely together during radon buildup. The same cannot be said about radon washout, with relatively large ranges for the predicted S_{on} and F. In contrast, sinusoidal diurnal variations can be easily observed during radon washout, especially in Fig. 4c and Fig. 4d, while the phenomenon was not as apparent during radon buildup, possibly masked over by the fluctuations in Fig. 3.

Both compartmental models fit very well with the observed data with all χ_r^2 close to one. This includes the new radon washout model, where the equation correctly follows the data well beyond the initial region. The chamber source term also increased significantly from S_{off} to S_{on}. This may indicate that the parameter is very sensitive to the pressure differential, as driven by the ventilation. The assumption of a constant source term also does not model the sinusoidal diurnal behavior. It may be ultimately possible to model the kinetics of S_{off} and S_{on} as a function of relevant environmental parameters if these are available.

Conclusions

This study evaluated the performance of five active radon monitors using an *RMSE* metric. Despite a dramatically lower list price, measurements from the RadonEye and RadonEye Plus2 both follow closely with the AlphaGUARD under the conditions of radon buildup, washout, and steady-state. Although having substantially limited functionality, the RadonEye and RadonEye Plus2 are good alternative to other more expensive equipment for many applications. The AlphaGUARD experienced significant fluctuations from the other monitors at higher radon concentrations. Though causes of the phenomenon are unclear and require further experimentation, impact on the conclusions should be minimal, as most of the devices were calibrated using average AlphaGUARD measurements over larger sampling intervals, where fluctuations were no longer observed.

Data from the five devices fit very well with the two compartmental models for ventilation buildup and washout, especially for RadonSentinel, which nominally outperformed the AlphaGUARD for this experiment. With the newly proposed washout model, data were accurately fit beyond the initial region. The chamber source term was significantly increased compared to other time periods, possibly resulting from a change in indoor-outdoor pressure differential. For a more accurate model that reflects cyclic diurnal variations, the source term may ultimately be modelled as a function of time and other environmental parameters using methods involving artificial intelligence or computational fluid dynamics analysis.

References

Burghele B, Cosma C. Intercomparison between radon passive and active measurements and problems related to thoron measurements. Rom J Phys 58:S56–S61; 2013.

Cardellini F, Chiaberto E, Garlati L, Giuffrida D, Leonardi F, Magnoni M, Minchillo G, Prandstatter A, Serena E, Trevisi R, Tripodi R, Veschetti M. Main results of the international intercomparison of passive radon detectors under field conditions in Marie Curie's tunnel in Lurisia (Italy). Nukleonika 61(3):251–256; 2016. DOI: 10.1515/nuka-2016-0042.

Chung LK, Mata LA, Carmona MA, Shubayr NAM, Zhou Q, Ye Y, Kearfott KJ. Radon kinetics in a natural indoor radon chamber. Sci Total Environ 734(139167):1–8; 2020. DOI: 10.1016/j.scitotenv.2020.139167.

Gunning GA, Murray M, Long SC, Foley MJ, Finch EC. Inter-comparison of radon detectors for one to four week measurement periods. J Radiol Prot 36(1):104; 2016. DOI: 10.1088/0952-4746/36/1/104.

Janik M, Tokonami S, Kranrod C, Sorimachi A, Ishikawa T, Hassan NM. International intercomparisons of integrating radon/thoron detectors with the NIRS radon/thoron chambers. Radiat Prot Dosim 141(4):436–439; 2010. DOI: 10.1093/rpd/ncq230.

Kanse SD, Sahoo BK, Sapra BK, Gaware JJ, Mayya YS. Powder sandwich technique: a novel method for determining the thoron emanation potential of powders bearing high ^{224}Ra content. Radiat Meas 48:82–87; 2013. DOI: 10.1016/j.radmeas.2012.10.014.

Kearfott KJ. Preliminary experiences with ^{222}Rn gas in Arizona homes. Health Phys 56(2):169–179; 1989. DOI: 10.1097/00004032-198902000-00004.

Keith S, Doyle JR, Harper C, Mumtaz M, Tarrago O, Wohlers DW, Diamond GL, Citra M, Barber LE. Analytical methods. In: Toxicological profile for radon. Atlanta, GA: Agency for Toxic Substances & Disease Registry; 2012:147–158.

Kuo T, Tsunomori F. Estimation of fracture porosity using radon as a tracer. J Petrol Sci Eng 122:700–704; 2014. DOI: 10.1016/j.petrol.2014.09.012.

Lederer CM, Shirley VS, eds. Table of isotopes. 7th ed. New York, NY: John Wiley and Sons; 1978.

Legates DR, McCabe GJ Jr. Evaluating the use of "goodness-of-fit" measures in hydrologic and hydroclimatic model validation. Water Resour Res 35(1):233–241; 1999. DOI: 10.1029/1998WR900018.

Lehnert AL, Kearfott KJ. An equilibrium-based model for measuring environmental radon using charcoal canisters. Health Phys 99(Suppl 2):S154–S163; 2010. DOI: 10.1097/HP.0b013e3181d966ad.

Lin C, Kuo T, Fan K, Chen Y, Su C, Tong L, Lee C, Hu K, Liu C, Liang H, Tsai C, Chiang C. Characterization of well skin using buildup test and radon as a tracer. J Petrol Sci Eng 78(2):201–207; 2011. DOI: 10.1016/j.petrol.2011.07.009.

McGregor D, Shultis JK. Radiation detection: concepts, methods, and devices. 1st ed. Boca Raton, FL: CRC Press; 2020.

National Council on Radiation Protection and Measurements. Ionizing radiation exposure of the population of the United States. Bethesda, MD: NCRP; NCRP Report No. 160; 2009.

Papp B, Cosma C, Cucos A. International intercomparison exercise of active radon devices and passive detectors at the First East European Radon Symposium (FERAS 2012). Rom Rep Phys 69(702):1–10; 2017.

Ritter A, Munoz-Carpena R. Performance evaluation of hydrological models: statistical significance for reducing subjectivity in goodness-of-fit assessments. J Hydrol 480:33–45; 2013. DOI: 10.1016/j.jhydrol.2012.12.004.

Tanaka A, Minami N, Yasuoka Y, Iimoto T, Omori Y, Nagahama H, Muto J, Mukai T. Accurate measurement of indoor radon concentration using a low-effective volume radon monitor. Radiat Prot Dosim 177(3):324–330; 2017. DOI: 10.1093/rpd/ncx050.

Taylor JR. An introduction to error analysis: the study of uncertainties in physical measurements. 2nd ed. Sausalito, CA: University Science Books; 1997.

Turk M, Volaric B, Antolkovic B. Radon activity concentration in the ground and its correlation with the water content of the soil. Appl Radiat Isotopes 47(3):377–381; 1996. DOI: 10.1016/0969-8043(95)00307-X.

World Health Organization (WHO). Handbook on indoor radon: a public health perspective. Geneva: WHO Press; 2009.

Xie D, Liao M, Kearfott KJ. Influence of environmental factors on indoor radon concentration levels in the basement and first floor of a building—a case study. Radiat Meas 82:52–58; 2015. DOI: 10.1016/j.radmeas.2015.08.008.

Xie D, Liao M, Hanqing W, Kearfott KJ. A study of diurnal and short-term variations of indoor radon concentrations at the University of Michigan, USA, and their correlations with environmental factors. Indoor Built Environ 26:1051–1061; 2017. DOI: 10.1177/1420326X16660755.

Yarmoshenko I, Malinovsky G, Vasilyev A, Zhukovsky M. Method for measuring radon flux density from soil activated by a pressure gradient. Radiat Meas 119:150–154; 2018. DOI: 10.1016/j.radmeas.2018.10.011.

Ye Y, Chung LK, Zhou Q, Kearfott KJ. Evaluation of ^{222}Rn and ^{220}Rn discriminating concentration measurements with pinhole-based twin cup dosimeters using computational fluid dynamics simulations. Radiat Meas 134(106369):1–7; 2020. DOI: 10.1016/j.radmeas.2020.106369.

Zafrir H, Barbosa SM, Malik U. Differentiation between the effect of temperature and pressure on radon within the subsurface geological media. Radiat Meas 49:39–56; 2013. DOI: 10.1016/j.radmeas.2012.11.019.

List of Figure Captions

Figure 1: Schematic of the basement space, with location of radon monitors and fans. All dimensions in meters.

Figure 2: Steady-state radon concentration measurements by the five devices over a) initial 24-h steady-state period, b) 9-d buildup period with fans turned off and double steel doors closed, and c) 24-h washout period with fans turned on and double steel doors opened.

Figure 3: Radon concentration measurements as dots and best-fit compartmental model as a solid line during buildup for (a) AlphaGUARD, (b) AB-5, (c) RadonEye, (d) RadonEye Plus2, and (e) RadonSentinel, after fans were turned off and double steel doors were closed for nine days.

Figure 4: Radon concentration measurements as dots and best-fit compartmental model as a solid line during washout for (a) AlphaGUARD, (b) AB-5, (c) RadonEye, (d) RadonEye Plus2, and (e) RadonSentinel, with fans turned on and double steel doors opened for 24 h.

Table 1

Table 1: Specifications of the active radon devices used in the experiment, as reported by manufacturers or by a commercial laboratory.

Company	Device	Price (USD)	Memory (points)	Battery	Accuracy	Sensitivity (cpm Bq^{-1} m^3)	Range (Bq m^{-3})	Measurement Interval Used
Saphymo	AlphaGURAD	$10,000	4,800	10 d	3%	0.05	2-2,000,000	10 min
Pylon	AB-5	Not reported	680	8 h	Not reported	0.03203	Not reported	10 min
RadonFTLab	RadonEye	$180	8,760	-	10%	0.0135	7-3,700	1 h
RadonFTLab	RadonEye Plus2	$180	8,760	-	10%	0.01	7-9,435	1 h
Sun Nuclear	RadonSentinel	$1,200	1,000	300 h	20%	0.0068	1-99,990	30 min

Table 2

Table 2: Results of the experiment and the devices' compatibility with first-order compartmental models and the "gold standard", AlphaGUARD.

		Steady-State		Buildup				Washout			
Company	Device	$\bar{X}$	*RMSE* (Bq m^{-3})	*L* (h^{-1})	S_{off} (Bq m^{-3} h^{-1})	χ_r^2	*RMSE* (Bq m^{-3})	S_{on} (Bq m^{-3} h^{-1})	*F* (h^{-1})	χ_r^2	*RMSE* (Bq m^{-3})
Saphymo	AlphaGUARD	1	-	0.015	45	5.50	-	142	0.54	10.31	-
Pylon	AB-5	0.78	166	0.016	44	2.11	168	136	0.61	8.15	78
RadonFTLab	RadonEye	0.97	76	0.013	42	2.42	80	70	0.27	5.49	66
RadonFTLab	RadonEye Plus2	0.93	81	0.013	42	2.80	75	60	0.27	8.15	38
Sun Nuclear	RadonSentinel	0.91	121	0.013	42	1.14	106	91	0.32	2.89	139

Figure 1 Click here to access/download;Figure;Fig1.png

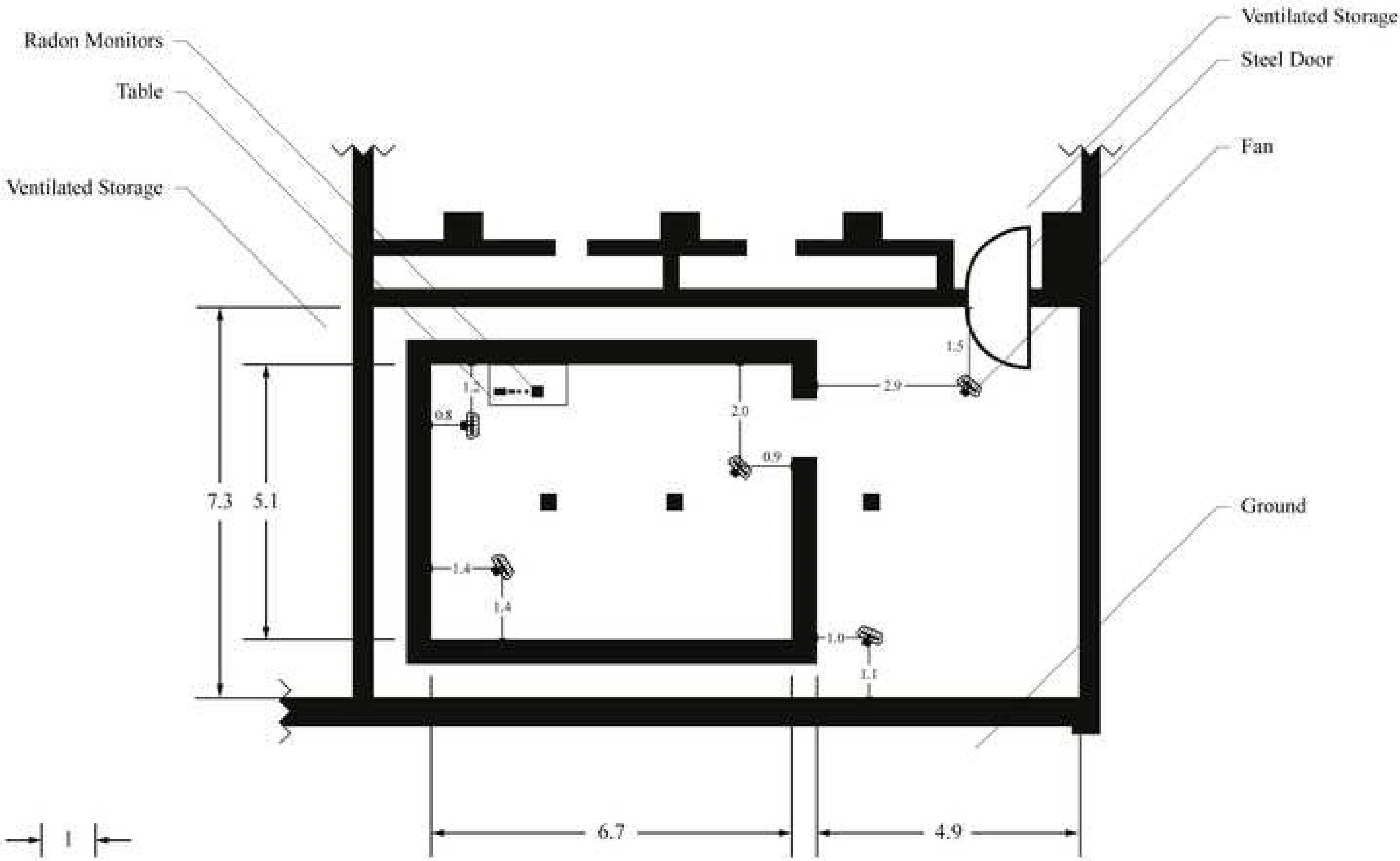

Figure 2a

Click here to access/download;Figure;Fig2a color.png

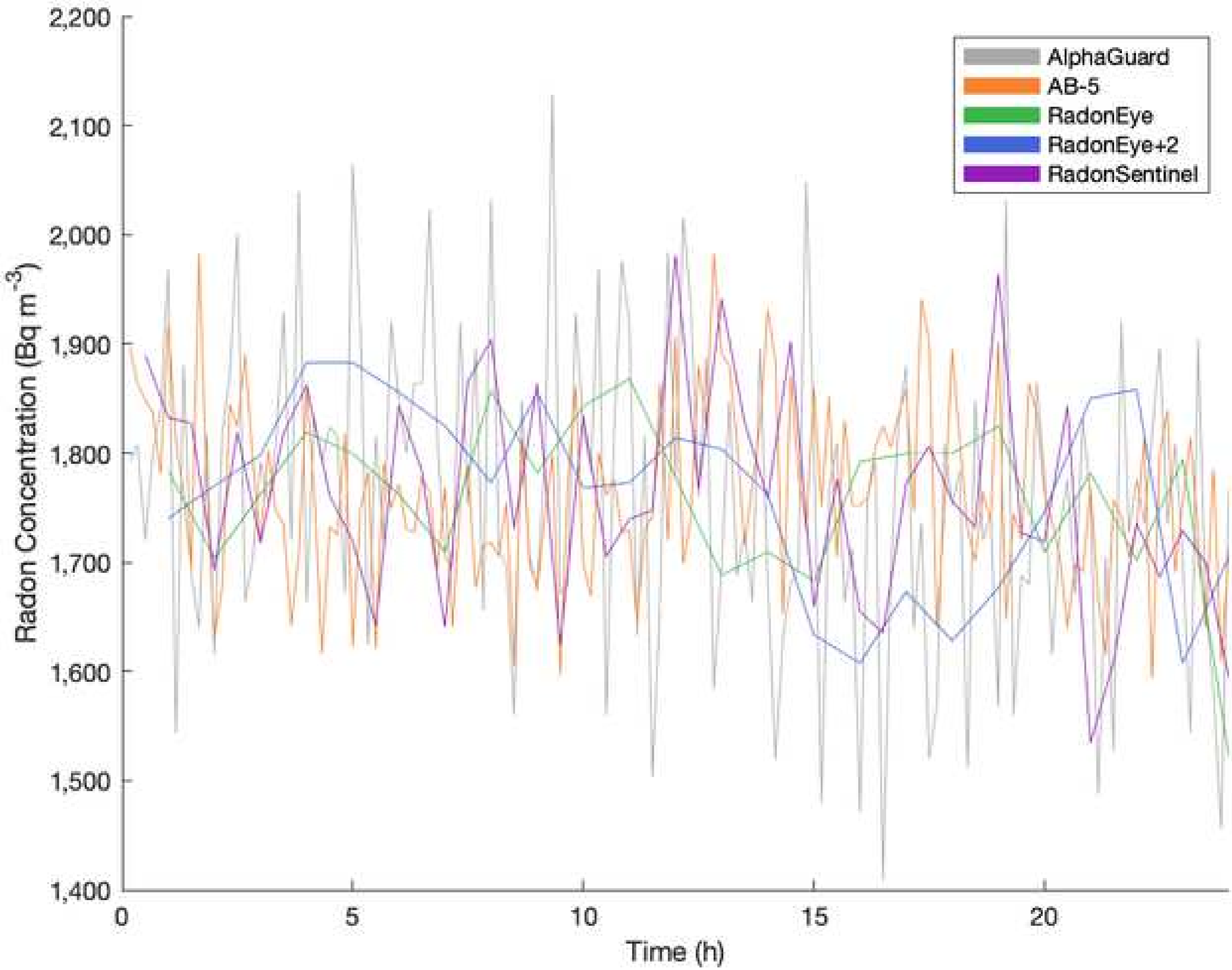

Figure 2b

Click here to access/download;Figure;Fig2b color.png

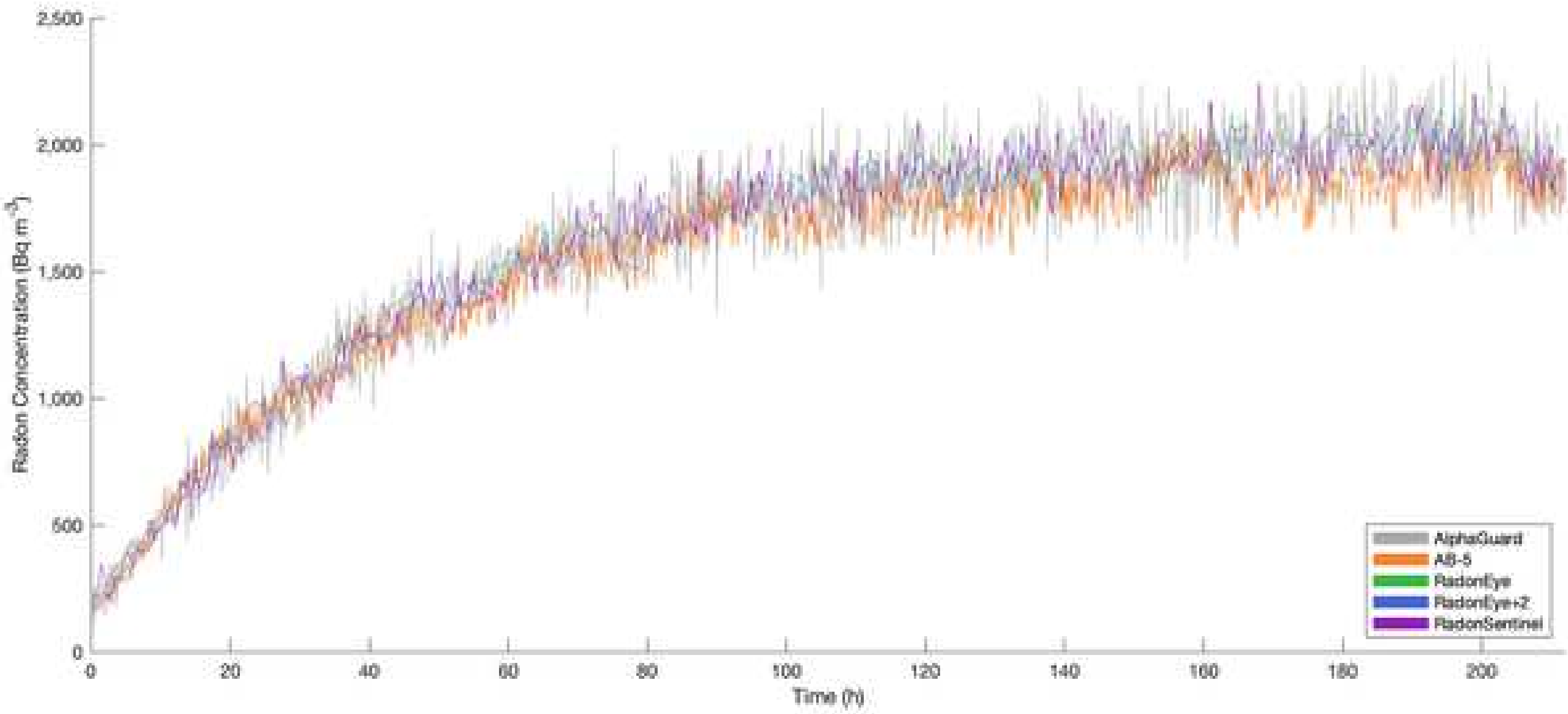

Figure 2c

Click here to access/download;Figure;Fig2c color.png

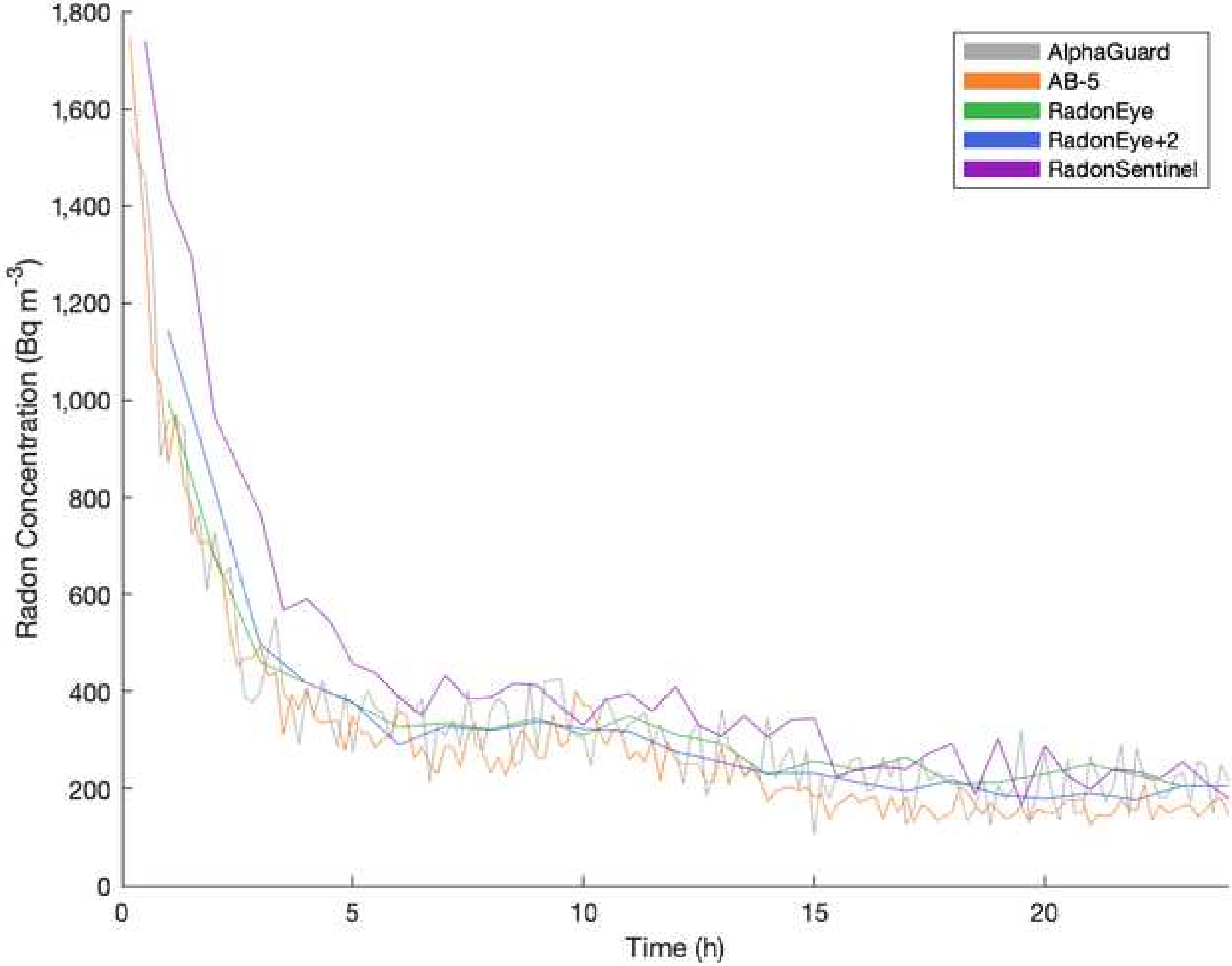

Figure 3a

Click here to access/download;Figure;Fig3a.png

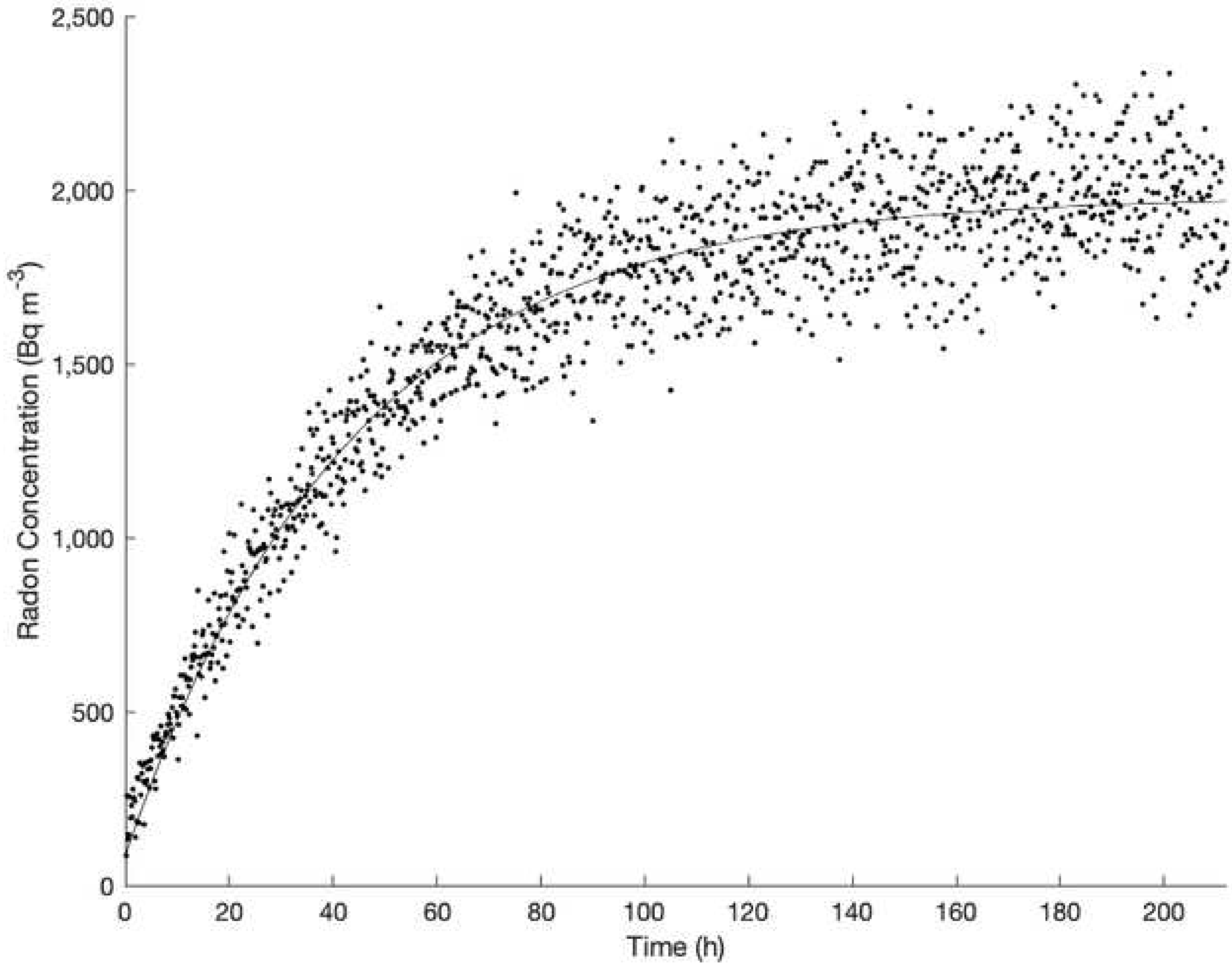

Figure 3b

Click here to access/download;Figure;Fig3b.png

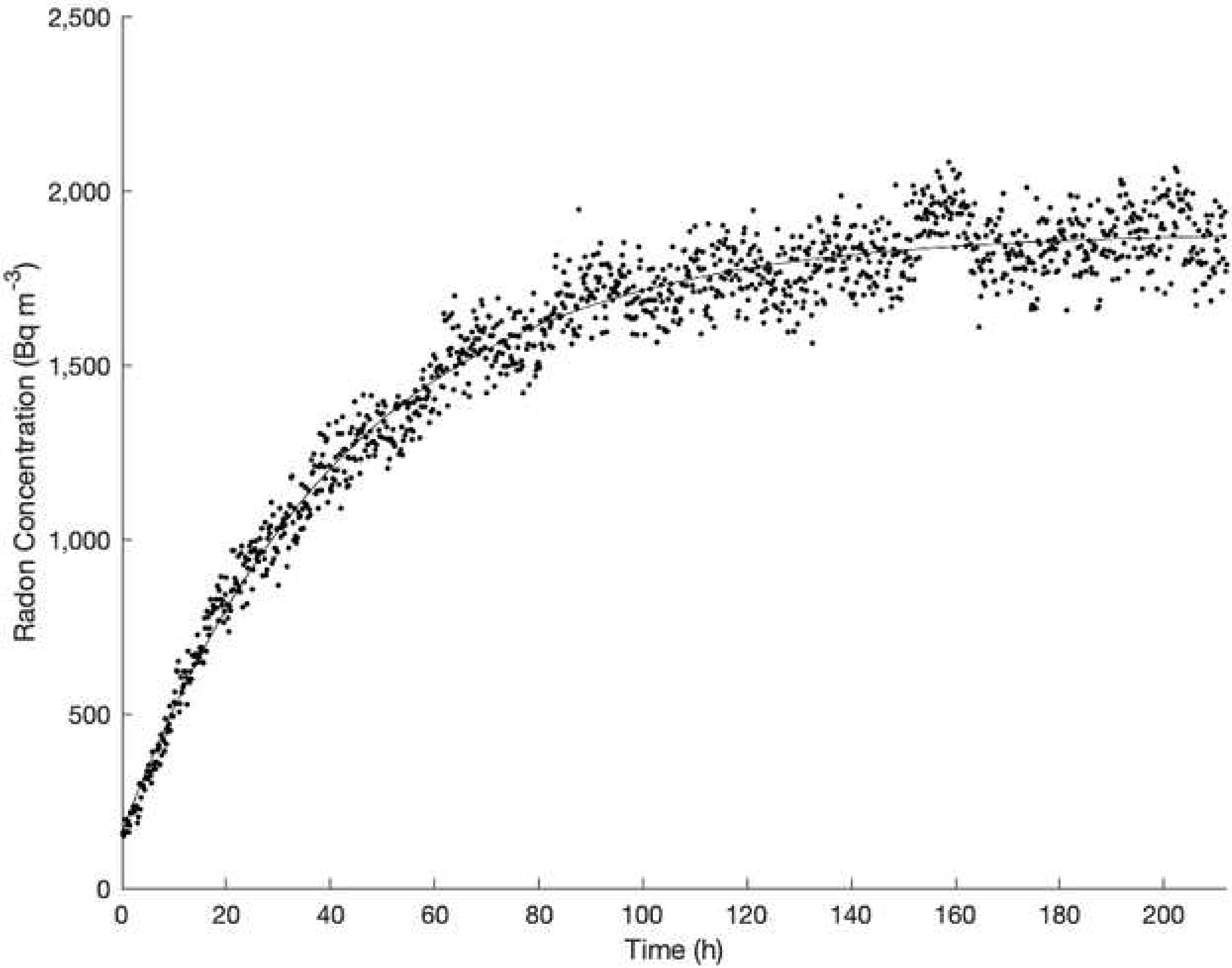

Figure 3c

Click here to access/download;Figure;Fig3c.png

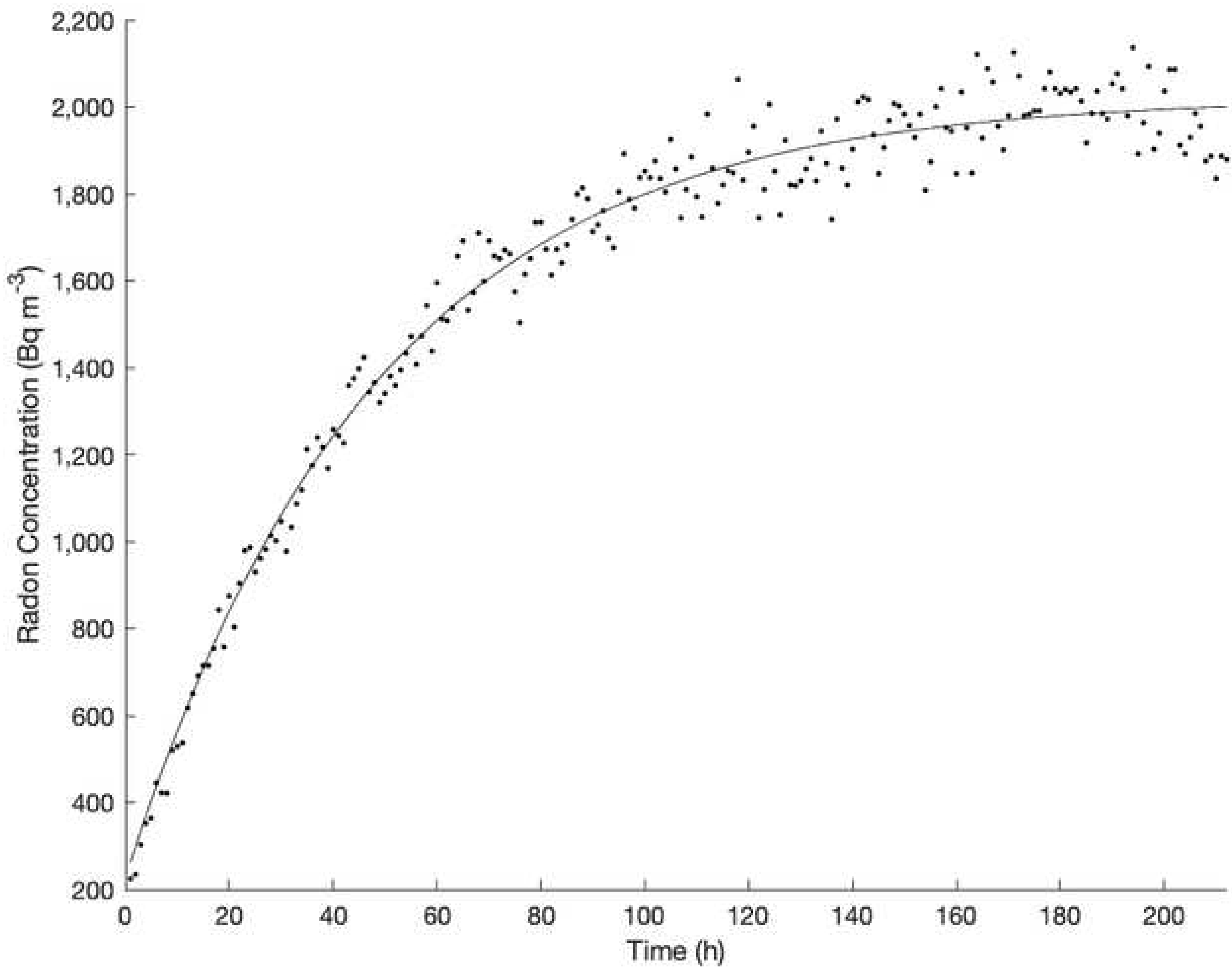

Figure 3d

Click here to access/download;Figure;Fig3d.png

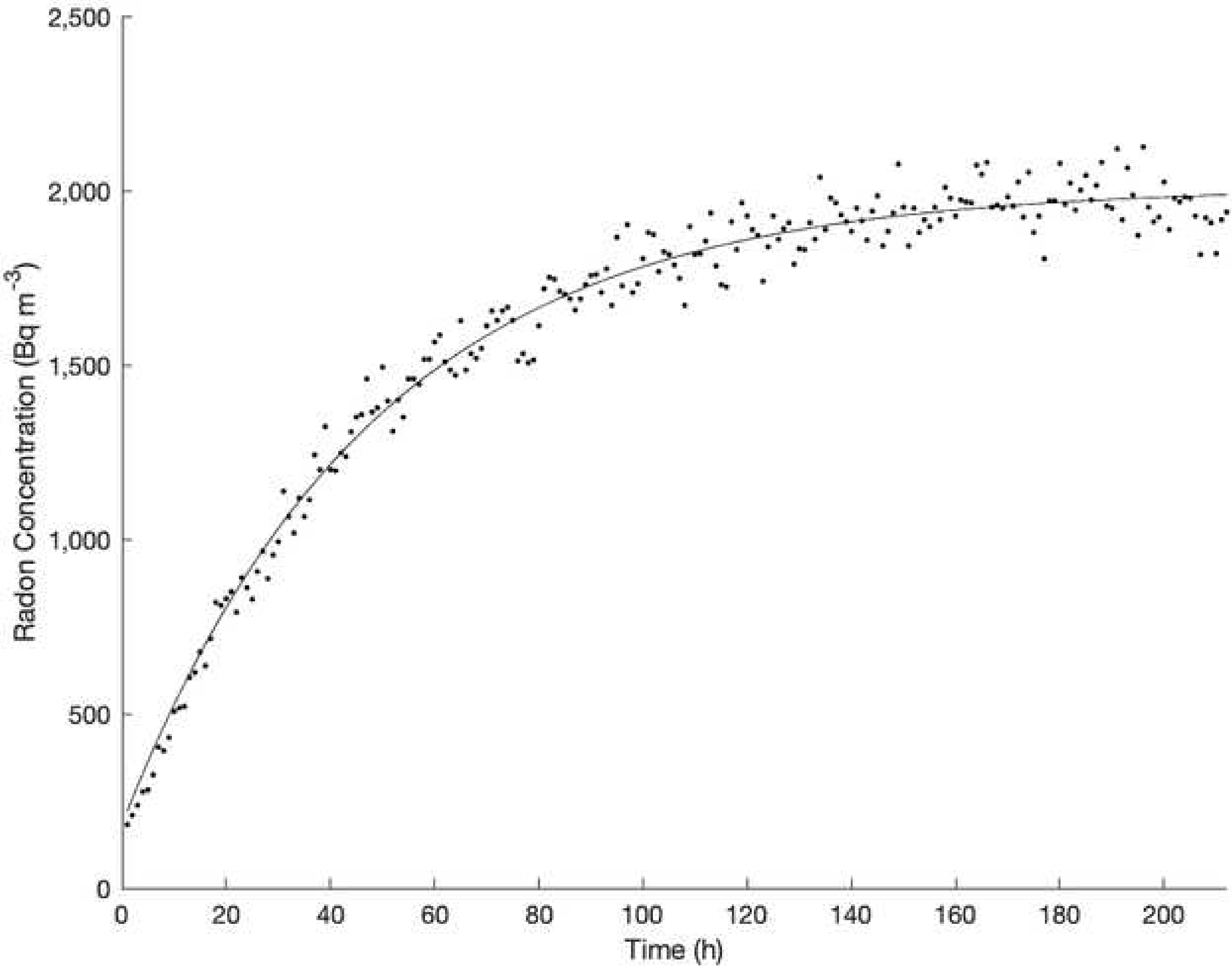

Figure 3e

Click here to access/download;Figure;Fig3e.png

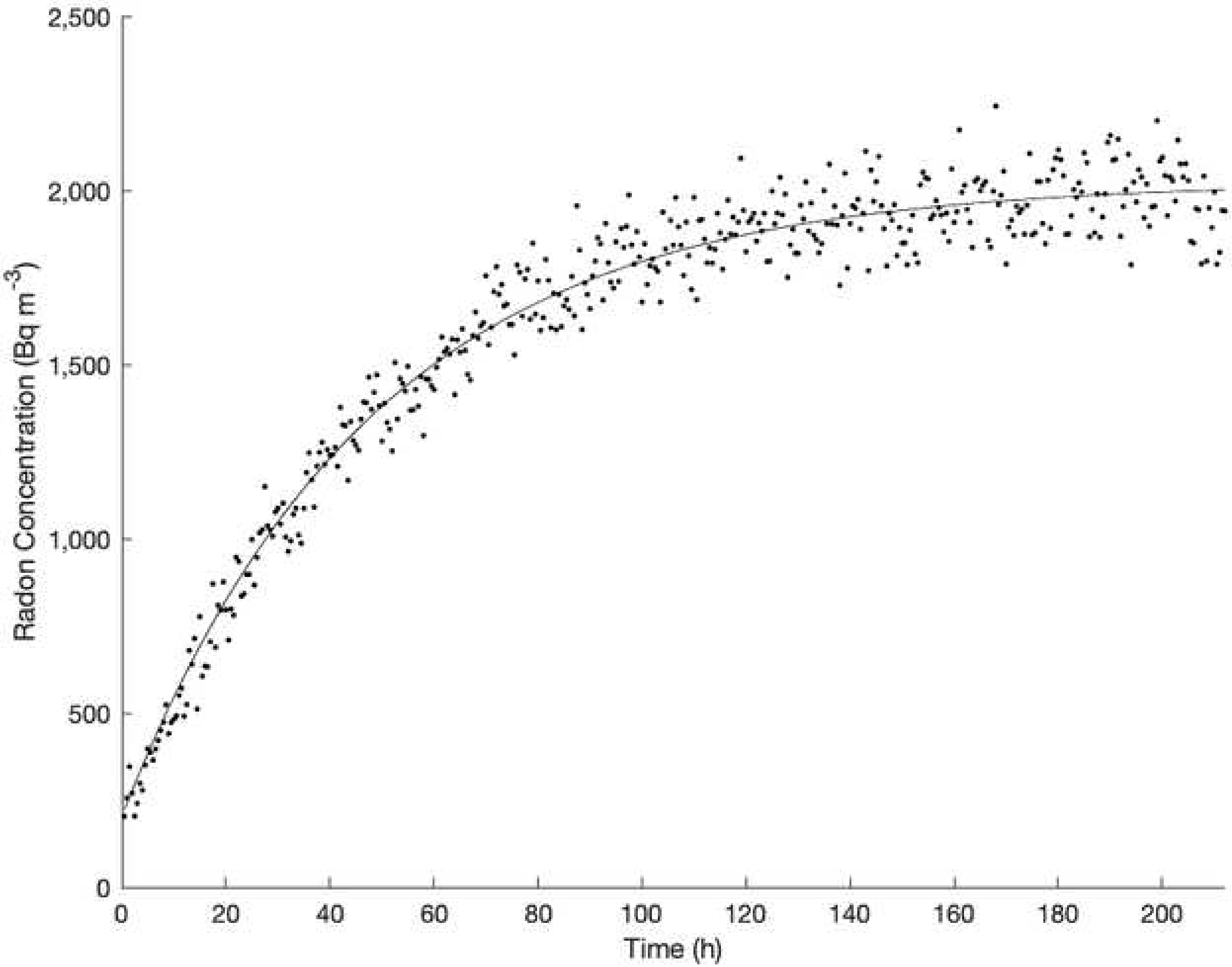

Figure 4a

Click here to access/download;Figure;Fig4a.png

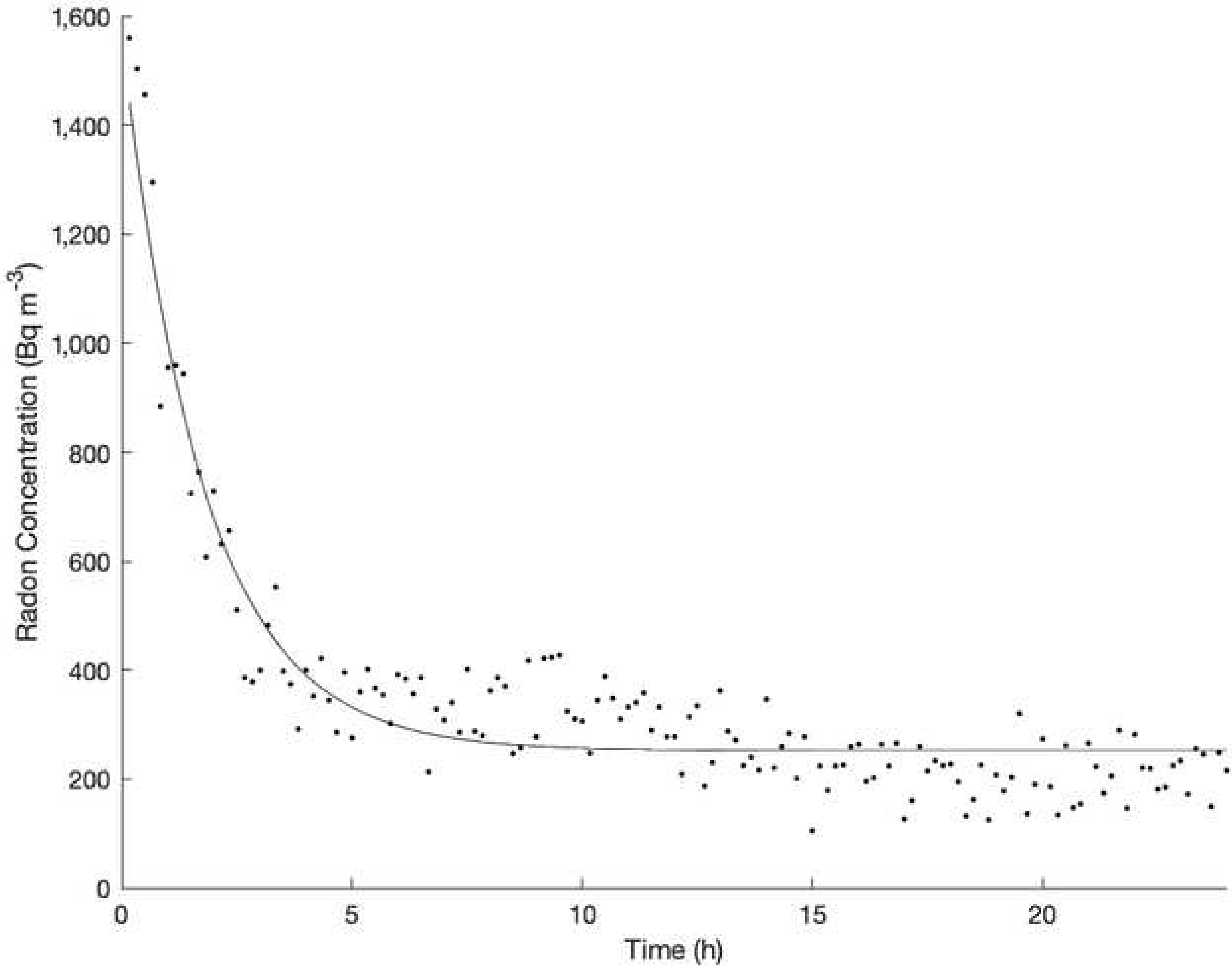

Figure 4b

Click here to access/download;Figure;Fig4b.png

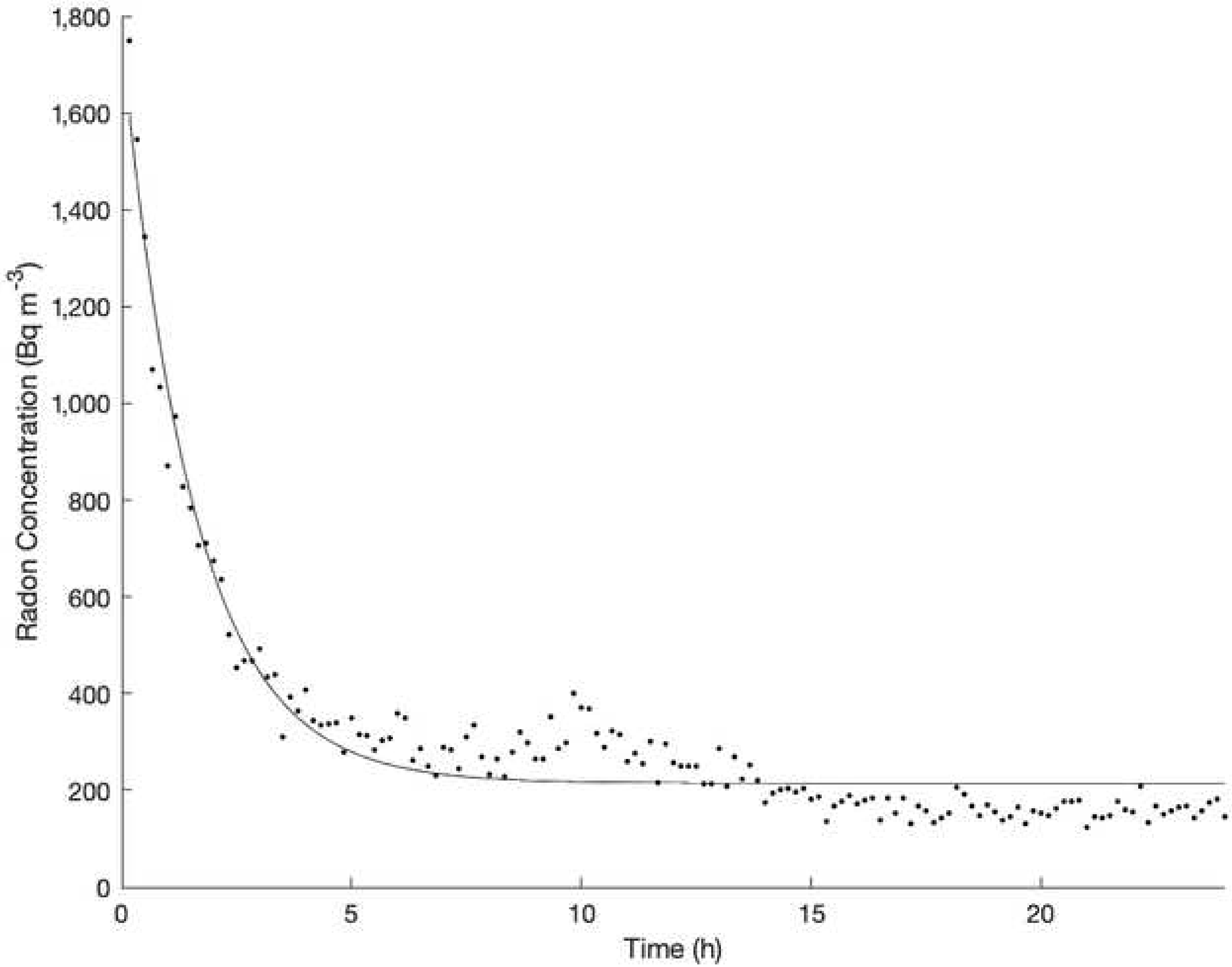

Figure 4c

Click here to access/download;Figure;Fig4c.png

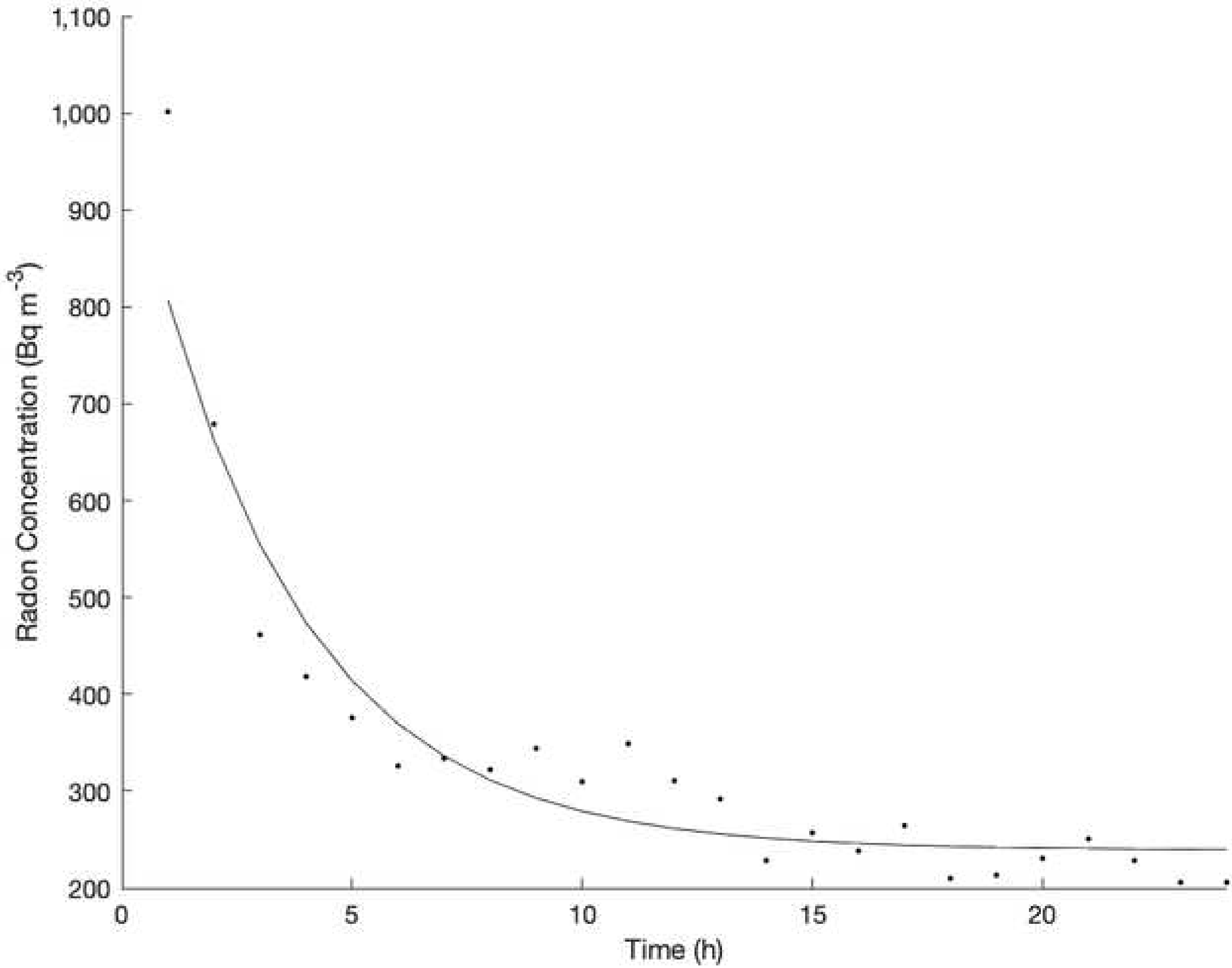

Figure 4d

Click here to access/download;Figure;Fig4d.png

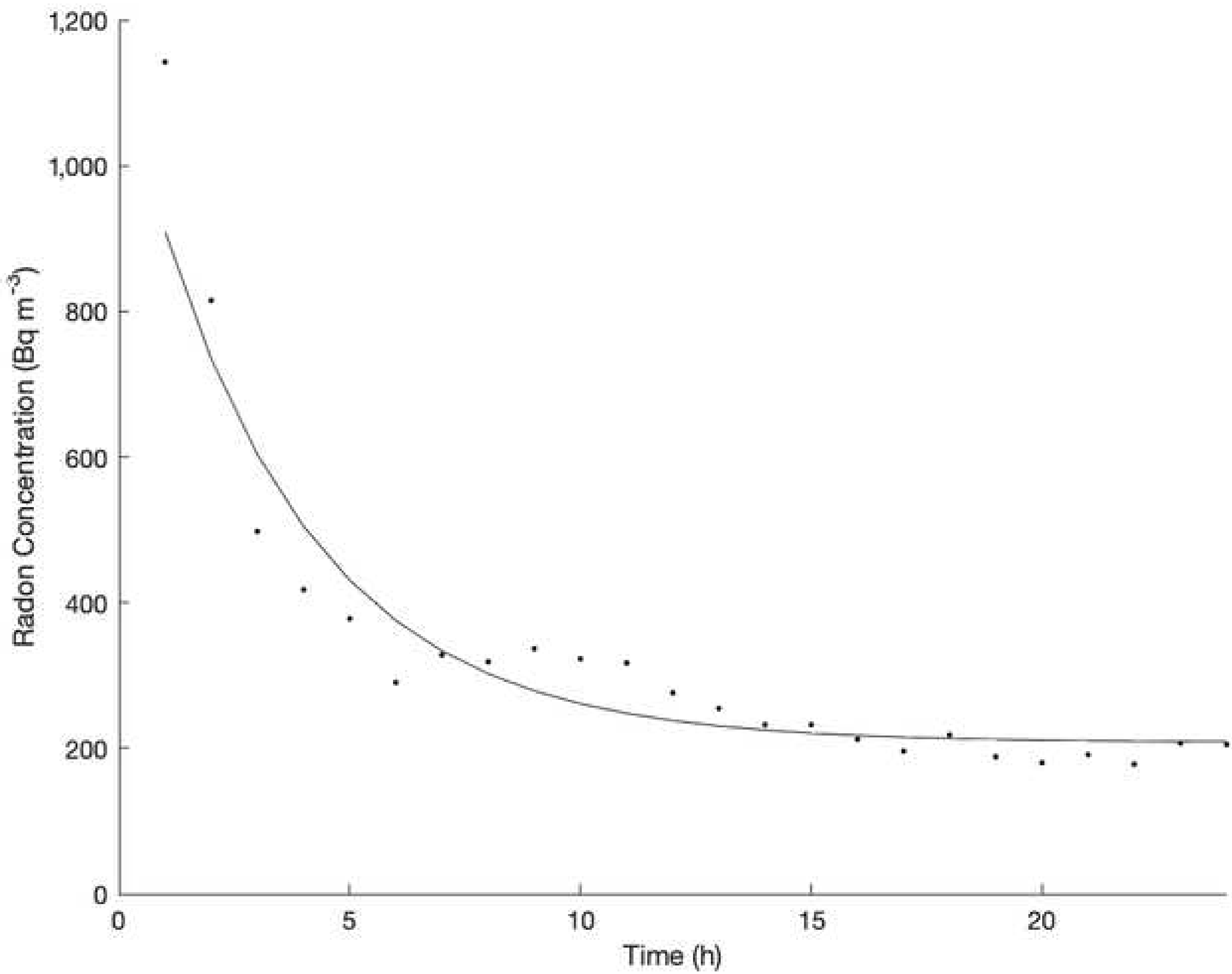

Figure 4e

Click here to access/download;Figure;Fig4e.png

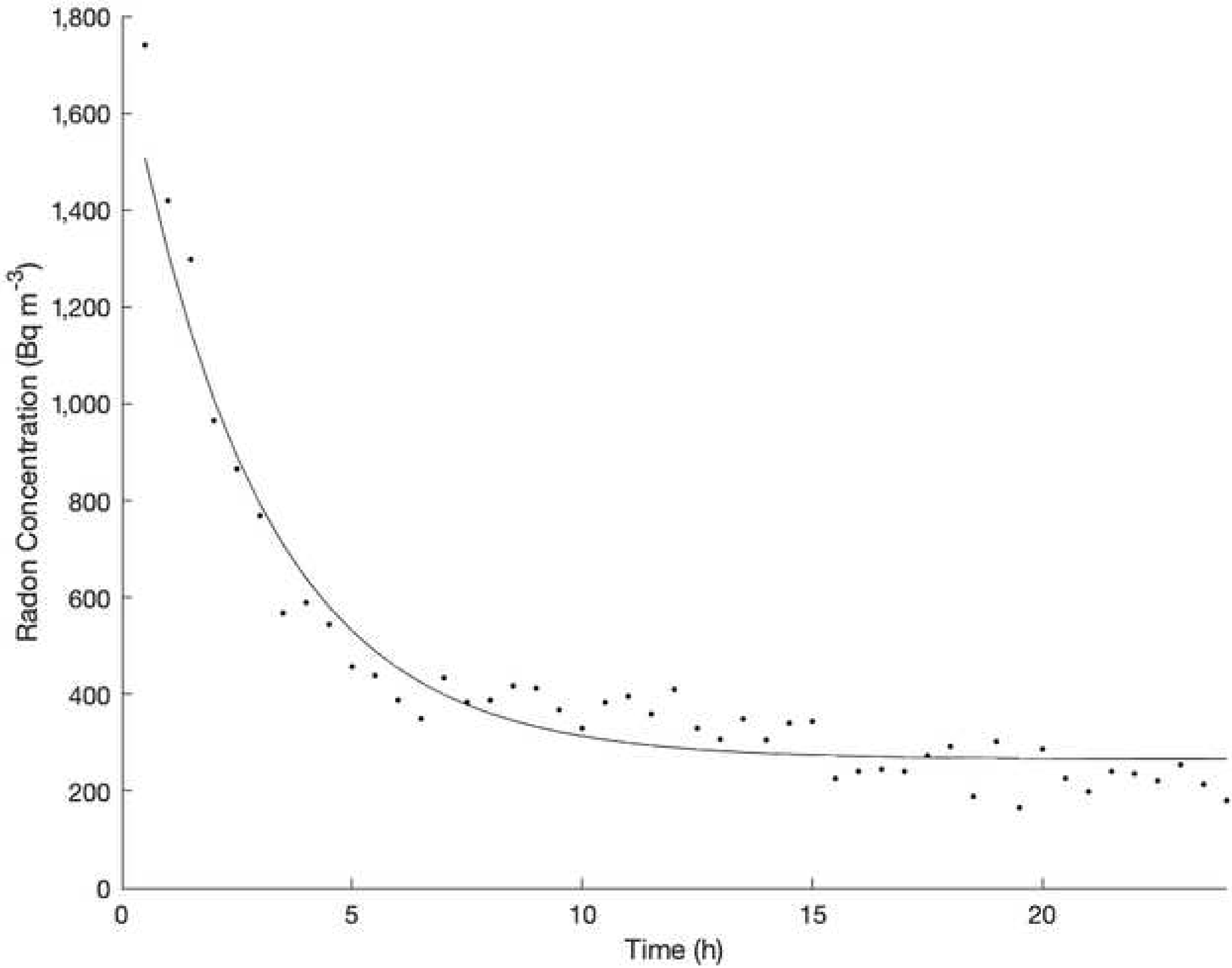

Long Kiu Chung is currently pursuing his master's degree in Mechanical Engineering at Stanford University. He received his bachelors in Mechanical Engineering from the University of Michigan in 2020. His email is edgarclk@umich.edu.

Author Photograph

Click here to access/download;Author Photograph;Chung_Headshot.jpg